In-Plane Optical and Electrical Anisotropy of 2D Black-Arsenic

Mianzeng Zhong[1], Haotong Meng[1], Sijie Liu[1], Huai Yang[2], Wanfu Shen[3], Chunguang Hu[3], Juehan Yang[2], Zhihui Ren[2], Bo Li[4], Yunyan Liu[5], Jun He[1*], Qinglin Xia[1*], Jingbo Li[6], and Zhongming Wei[2*]

[1]Hunan Key Laboratory of Super-microstructure and Ultrafast Process, School of Physics and Electronics, Central South University, Changsha 410083, Hunan, China

[2]State Key Laboratory of Superlattices and Microstructures, Institute of Semiconductors, Chinese Academy of Sciences & Center of Materials Science and Optoelectronics Engineering, University of Chinese Academy of Sciences, Beijing 100083, China

[3]State Key Laboratory of Precision Measuring Technology and Instruments, Tianjin University, Tianjin 300072, China

[4]Department of Applied Physics, School of Physics and Electronics, Hunan University, Changsha 410082, Hunan, China

[5]School of Physics and Optoelectronic Engineering, Shandong University of Technology, Zibo 255049, Shandong, China

[6]Institute of Semiconductors, South China Normal University, Guangzhou 510631, China

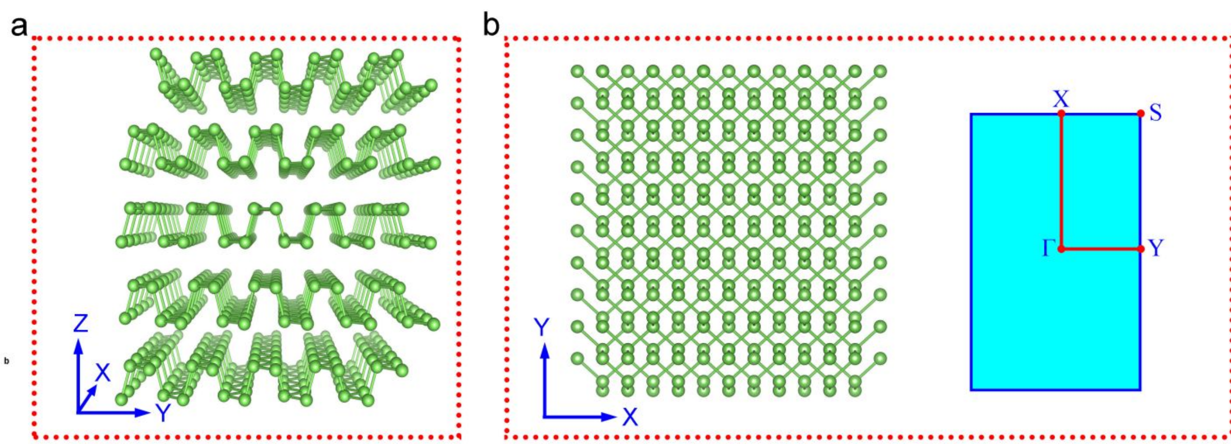

Figure S1. Crystal structures of orthorhombic b-As from (a) side view and (b) top view, showing its highly anisotropic nature.

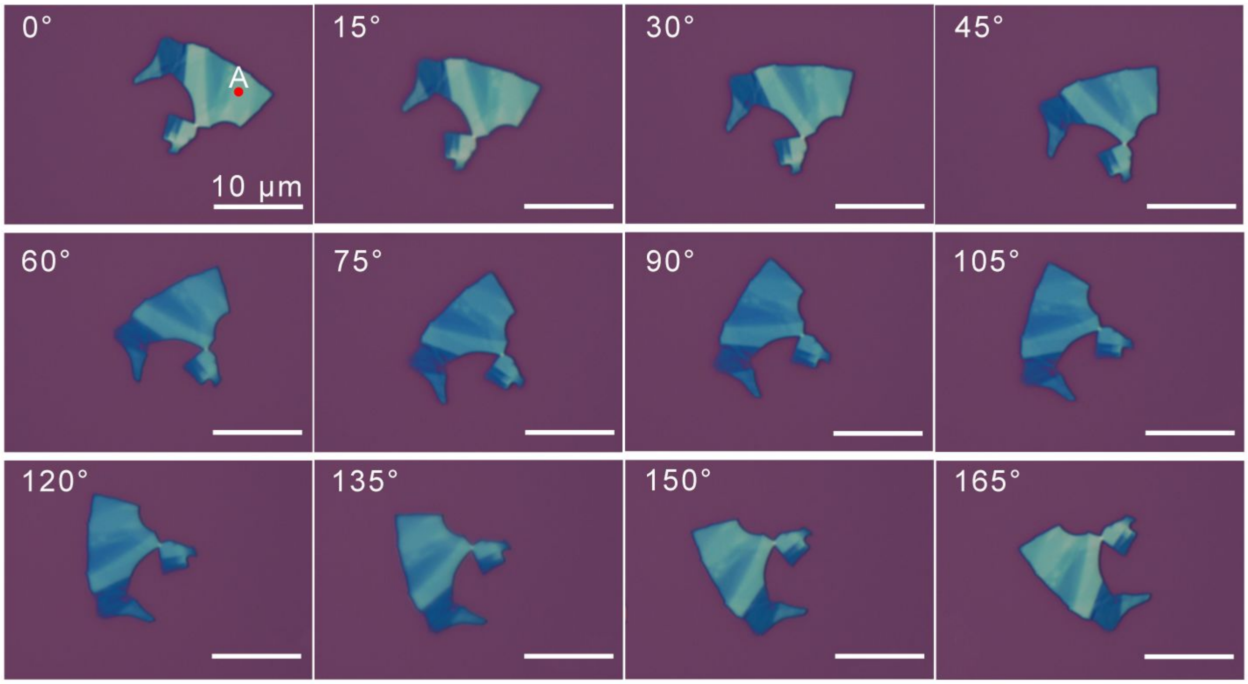

Figure S2. Polarization-resolved optical images of b-As flake.

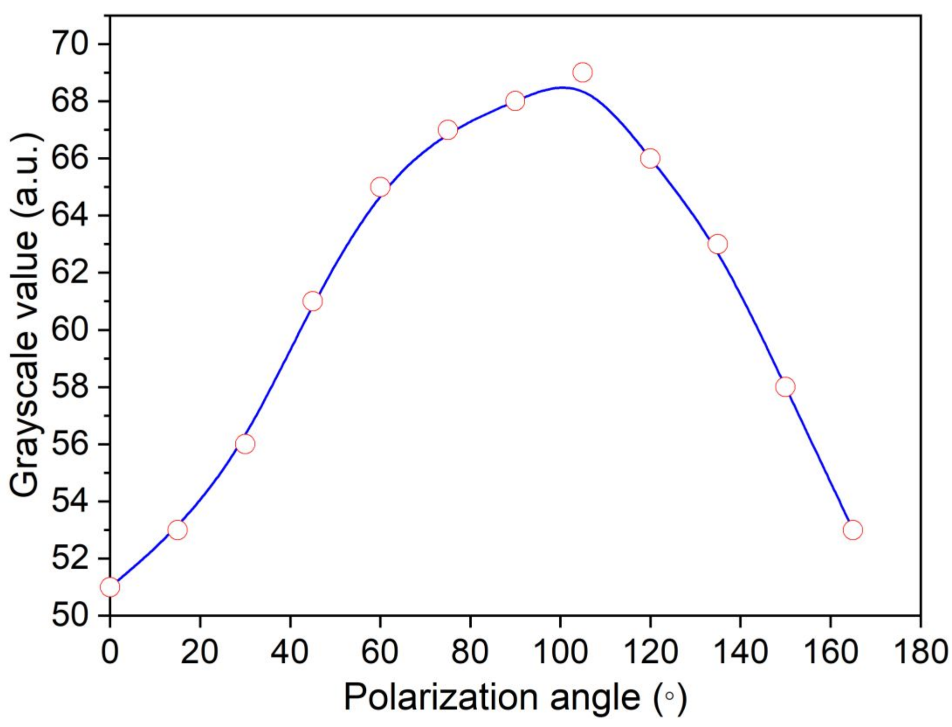

Figure S3. Grayscale values obtained from the A point in Figure S1 under different polarization angles as a function of the polarization angle.

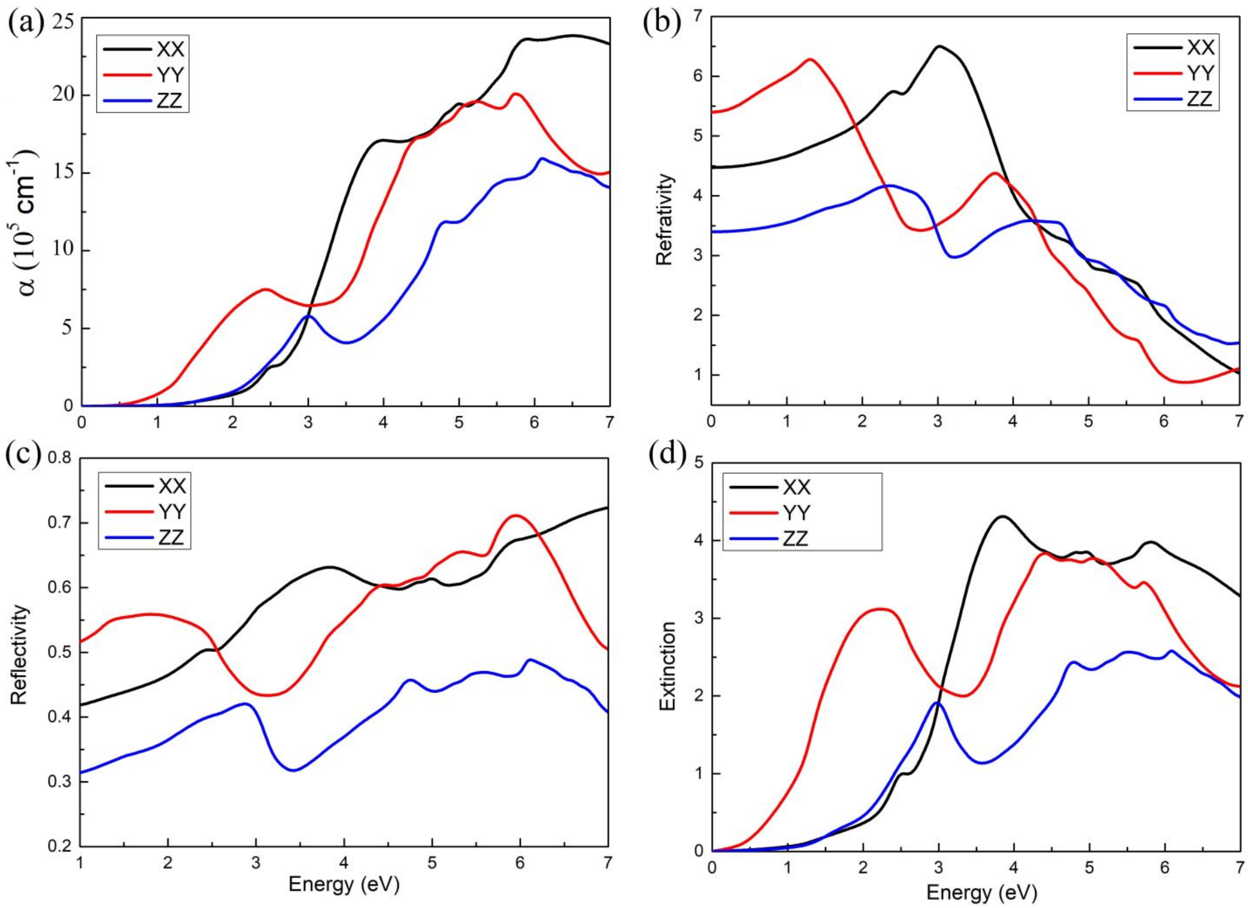

Figure S4. The absorption(a), reflectivity(b), refractive index (c), and extinction (d) for b-As considering XX, YY and ZZ directions.

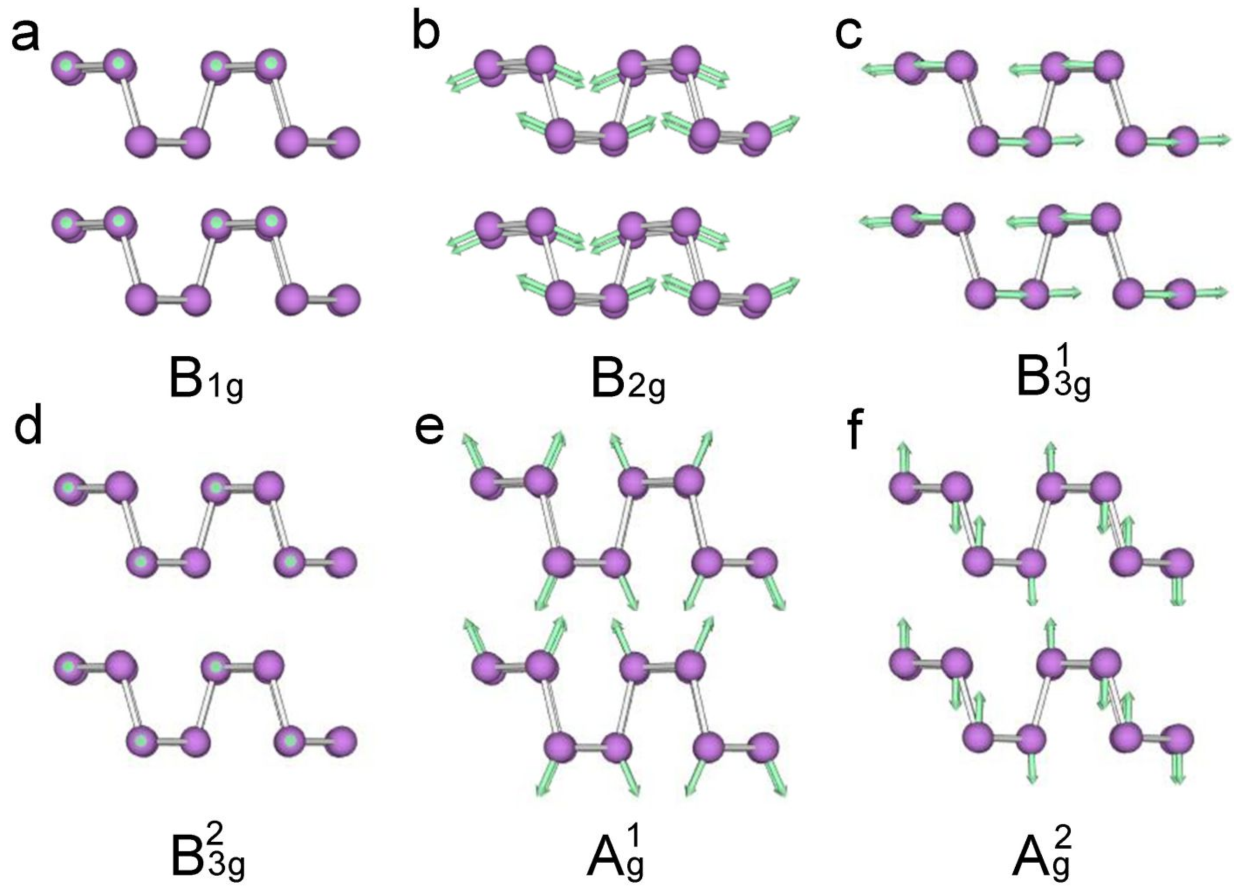

Figure S5. Schematic diagrams for six Raman-active modes in b-As. Green arrows indicate atomic displacements.

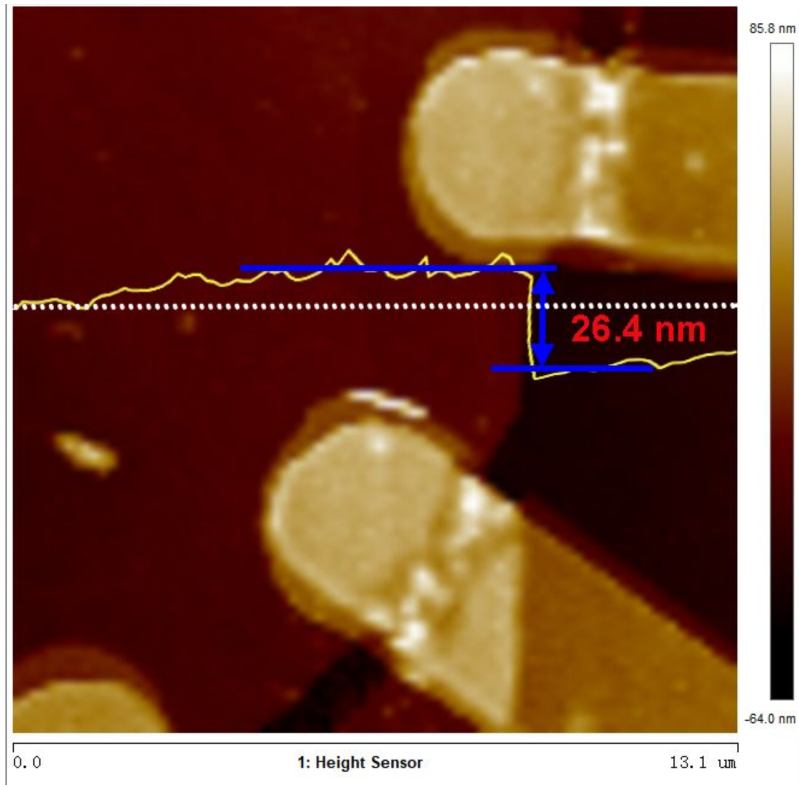

Figure S6. Atomic force microscopy (AFM) image of this typical b-As FET, the thickness of the b-As crystal is about 26.4nm.

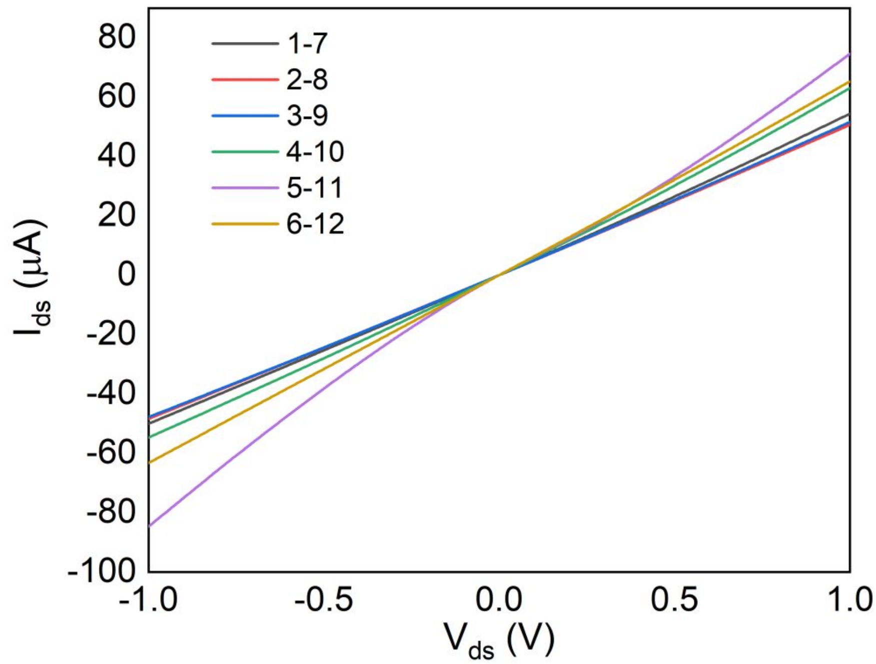

Figure S7. Room-temperature output characteristics (I_{ds}-V_{ds}) of this FET with the different directions (different symmetrical source-drain electrodes), the gate voltage is 0V.

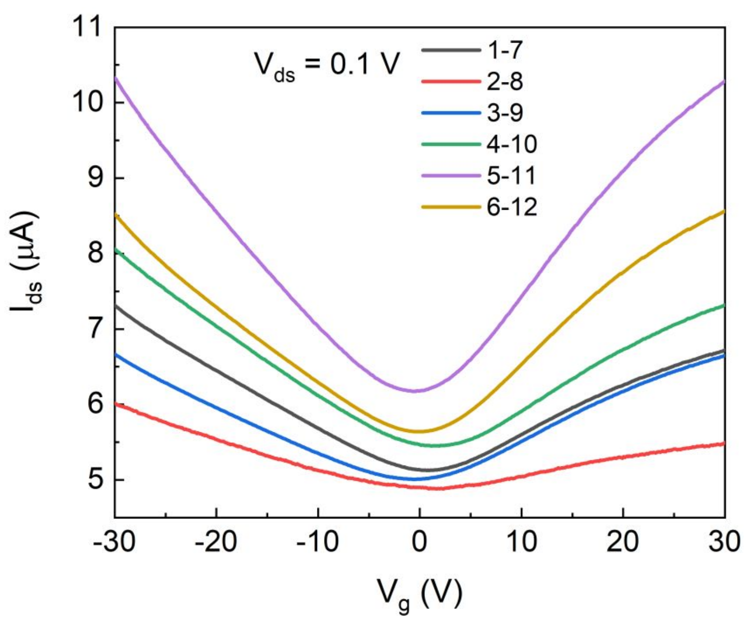

Figure S8. Room-temperature transfer characteristics (I_{ds}-V_g) of this FET with the different directions (different symmetrical source-drain electrodes), the drain-source voltage is 1V.

Note S1

For b-As, the Raman tensors of the phonons with A_g, and B_{2g} symmetry are

$$\overleftrightarrow{R}_{A_g} = \begin{pmatrix} a & 0 & 0 \\ 0 & b & 0 \\ 0 & 0 & c \end{pmatrix} = \begin{pmatrix} |a|e^{i\emptyset_a} & 0 & 0 \\ 0 & |b|e^{i\emptyset_b} & 0 \\ 0 & 0 & |c|e^{i\emptyset_c} \end{pmatrix} \quad \text{(S1)}$$

and

$$\overleftrightarrow{R}_{B_{2g}} = \begin{pmatrix} a & 0 & f \\ 0 & 0 & 0 \\ f & 0 & 0 \end{pmatrix} = \begin{pmatrix} 0 & 0 & |f|e^{i\emptyset_f} \\ 0 & 0 & 0 \\ |f|e^{i\emptyset_f} & 0 & 0 \end{pmatrix} \quad \text{(S2)}$$

where $|a|$, $\emptyset_a$, $|b|$, $\emptyset_b$, $|c|$, $\emptyset_c$, $|f|$, and $\emptyset_f$ are the magnitude and complex phase of the independent components of these two tensors, respectively. In our experimental configuration, the incident laser beam along the y direction (perpendicular to the layer plane of our arsenic sample). So, the polarization vector of the incident beam ($\hat{e}_i$) can be expressed as $\hat{e}_i = (\sin\theta \;\; 0 \;\; \cos\theta)$ (θ is the sample rotation angle), and the polarization vector of the scattered light ($\hat{e}_s$) can be expressed as $\hat{e}_s = (\sin\theta \;\; 0 \;\; \cos\theta)$ and $\hat{e}_s = (\cos\theta \;\; 0 \;\; -\sin\theta)$ for the parallel and cross-polarization configurations, respectively. The Raman scattering intensity, which is related to the Raman tensor and the polarization vectors of incident laser beam and scattered light, is expressed as $S \propto \left|\hat{e}_i \cdot \overleftrightarrow{R} \cdot \hat{e}_s\right|^2$. As a consequence, the Raman intensities of A_{1g} and B_{2g} modes under parallel and cross-polarization configurations are written as following

$$S_{A_g}^{//} = (|a|sin^2\theta + |c|cos\emptyset_{ca}cos^2\theta)^2 + |c|^2 sin^2\emptyset_{ca}cos^4\theta \qquad \text{(S3)}$$

$$S_{A_g}^{\perp} = [(|a| - |c|cos\emptyset_{ca})^2 + |c|^2 sin^2\emptyset_{ca}]cos^2\theta sin^2\theta \qquad \text{(S4)}$$

$$S_{B_{2g}}^{//} = |f|^2 sin^2 2\theta \qquad \text{(S5)}$$

$$S_{B_{2g}}^{\perp} = |f|^2 cos^2 2\theta \qquad \text{(S6)}$$

where $\emptyset_{ca}$ is the phase difference $\emptyset_c - \emptyset_a$. As described, the Raman intensity of A_{1g} and B_{2g} modes shows different periodic variation with the sample rotation angle under parallel and cross-polarization configurations of the scattered light. According to (3) and (5), under the parallel configuration, when the crystal orientation parallel to the scattered light, the Raman intensity of A_{1g} mode has maximum or minimum value, while B_{2g} mode is forbidden. In contrast, under the cross-polarization configuration, the A_{1g} mode is forbidden, and Raman intensity of B_{2g} mode has the maximum value.